

# Electrochemical Sensor based on Nano-Perovskite/Ionic Liquid Crystal Modified Carbon Paste Electrode for Effective Determination of Hydroquinone and Catechol

Ekram H. El-Ads, Nada F. Atta\*, Ahmed Galal, Nada A. Eid

Chemistry Department, Faculty of Science, Cairo University, 12613 Giza, Egypt

\*E-mail: [anada@sci.cu.edu.eg](mailto:anada@sci.cu.edu.eg)

Received: 14 October 2017 / Accepted: 8 December 2017 / Published: 28 December 2017

---

An effective and facile method for the simultaneous determination of dihydroxy-benzene isomers, hydroquinone "HQ" and catechol "CC", at NdFeO<sub>3</sub> nano-perovskite/ionic liquid crystal modified carbon paste electrode in presence of sodium dodecyl sulfate (NFILCCP-SDS) is introduced. The proposed nano-composite offered high current responses and low detection limits due to the inherent catalytic properties of its individual modifiers. The proposed sensor has high electro-catalytic activity toward simultaneous determination of HQ and CC in the linear dynamic range of 10 μmol L<sup>-1</sup> to 180 μmol L<sup>-1</sup> with correlation coefficients 0.989 and 0.989; detection limits of 0.118 μmol L<sup>-1</sup> and 0.252 μmol L<sup>-1</sup> and quantification limits of 0.392 μmol L<sup>-1</sup> and 0.840 μmol L<sup>-1</sup>, respectively. Three isomers; HQ, CC and resorcinol RC were simultaneously identified with good potential peaks separation. The determination of HQ and CC in presence of interfering species was also successful. Real sample analysis in tap water was achieved with acceptable recovery.

---

**Keywords:** Hydroquinone; Catechol; Tap water; NdFeO<sub>3</sub> perovskite; Carbon paste electrode.

## 1. INTRODUCTION

Hydroquinone "HQ" and catechol "CC", dihydroxy benzene isomers, have been widely used in different fields like cosmetics, dye, pesticides, antioxidants, medicines, flavoring agents, photography chemicals, pharmaceutical and chemical industries [1-3]. They are considered by the US Environment Protection Agency and the European Union as major environmental pollutants. They are highly toxic to both environment and humans even at their very low concentration. Also, they are difficult to degrade under the typical environmental conditions [1-8]. They might originate from different sources like factory effluents, waste water treatment, plants, agriculture, etc. [8-11].

Also, they could get inside the human body through digestive and respiratory systems and skin causing severe impacts for skin, mucosa and central nervous system [12-15]. On the other hand, HQ and CC show similar structures and properties so it is necessary to present a simple and rapid method for their simultaneous determination [16-18]. Different methods have been presented for this purpose including spectrophotometry, chromatography, fluorescence, chemiluminescence, and electrochemical methods [1, 2, 4, 8]. Electrochemical methods showed superior advantages compared to other methods like sensitivity, high efficiency, simplicity, no pretreatment steps, wide linear range, time saving analysis and low cost [2-4, 8]. Bare solid electrodes might lose the advantage of the simultaneous determination of HQ and CC due to their close oxidation potentials which resulted in overlapping of their voltammetry responses [2, 3, 8, 18]. Also, unmodified electrodes suffer from some drawbacks such as low sensitivity and reproducibility and slow electron transfer rate [4, 18, 19]. To overcome these drawbacks, modification of bare electrodes was achieved using different nanomaterials, transition metal compounds [3], ionic liquids [8], polymer films [18] and multiwalled carbon nanotubes [20-22].

Carbon paste electrode "CP" is considered as an important type of carbon-based electrodes with renewable surface. CP electrodes have been widely used in sensor applications due to their stable response, considerable life time, ease of fabrication, corrosion resistance and wide anodic and cathodic potential ranges [23-25]. Ionic liquid "IL" modified CP showed high conductivity, anti-fouling, good electro-catalytic activity and lower overpotential toward different studied compounds [26-30].

Ionic liquid crystals "ILCs", which compile the fascinating properties of ionic liquids ILs and liquid crystals, showed superior properties compared to ILs. ILCs, consisting of salts of cations and their counter ions, showed enhanced anisotropic conductivity and molecular orientational ordering [23, 26, 30]. One of the most common ILC is 2-chloro-1,3-dimethyl-imidazolium hexafluorophosphate containing imidazolium cation. This ILC showed good properties of chemical and electrochemical stability, low melting point and anisotropic ionic conductivity [23].

On the other hand, the modification of the ionic liquid crystal modified electrodes with nanomaterials offer more advantages over the traditionally ionic liquid modified electrodes involving enhanced stability, increased sensitivity and compatibility [23].

$ABO_3$  nano-perovskites have been widely used in different applications because of their electronic conductivity, mobility of oxide ions within the crystal, electrically active structure, variations of oxygen content, thermoelectric, magnetic, catalytic activity and thermal and chemical stability [31-33].  $NdFeO_3$  nano-oxide with 3D orthorhombic structure is considered one of the rare-earth orthoferrites group. There are three competing magnetic interactions between Nd–Nd, Nd–Fe and Fe–Fe affecting the structural and magnetic properties of  $NdFeO_3$ .  $NdFeO_3$  nano-perovskites have potential applications in catalysis, fuel cells, gas sensor and electrochemical sensor [26, 34-37].

Surfactants, amphiphilic compounds with hydrophilic head and hydrophobic tail, have found reflective impact in electrochemistry by improving the electrode/solution interface characteristics [1, 23, 30]. Surfactants can improve the electrochemical signal of the electroactive species, enhance the current response, selectivity, sensitivity and facilitate the electron transfer rate by reinforcing the accumulation/aggregation of the electroactive species at the electrode surface. Also, they can affect the

electrode processes in terms of redox potential and diffusion and charge transfer coefficients [1, 26, 30].

In the present work, we introduce an electrochemical sensor, NFILCCP-SDS, based on nano-perovskite  $\text{NdFeO}_3$ /ILC modified carbon paste electrode in presence of SDS. The aim is to use the fabricated sensor for the first time, in the sensitive determination of HQ and CC that are well known water-pollutants and used as ingredients in cosmetic industry. The electrochemical characteristics and figures of merits of the sensor will be presented.

## 2. EXPERIMENTAL

### 2.1. Materials and reagents

Catechol (CC), hydroquinone (HQ), resorcinol (RC), 2-chloro-1,3-dimethylimidazolium hexafluorophosphate ionic liquid crystal (ILC), 1-butyl-4-methylpyridinium tetrafluoroborate (IL1), 1-n-hexyl-3-methylimidazolium tetrafluoroborate (IL2), graphite powder, paraffin oil and sodium dodecyl sulfate (SDS) were purchased from Sigma Chemicals Co. The supporting electrolyte used in this work was 0.1 mol L<sup>-1</sup> phosphate buffer solution (PBS, consisting of 1 mol L<sup>-1</sup> K<sub>2</sub>HPO<sub>4</sub> and 1 mol L<sup>-1</sup> KH<sub>2</sub>PO<sub>4</sub>) of pH 2–9. pH was adjusted using 0.1 mol L<sup>-1</sup> H<sub>3</sub>PO<sub>4</sub> and 0.1 mol L<sup>-1</sup> KOH. Buffer solutions were stored in a refrigerator. Analytical grade chemicals and deionized water were used to prepare all solutions.

### 2.2. Instrumental and experimental set-up

#### 2.2.1. Electrochemical measurements

A standard three-electrode/one compartment glass cell was used for electrochemical characterizations. Carbon paste electrode (CP) with diameter of 6.3 mm and large surface area platinum electrode were used as the working and auxiliary electrodes, respectively. Ag/AgCl (4 mol L<sup>-1</sup> KCl saturated with AgCl) electrode was used as the reference electrode in all electrochemical studies. All experiments were carried out at 25 °C ± 0.2 °C. A BAS-100B electrochemical analyzer (Bioanalytical Systems, BAS, USA) controlled with a PC for experiment control, data acquisition and analysis was used for the electrochemical characterizations. Quanta FEG 250 instrument was used for the investigation of the microstructure of different samples.

#### 2.2.2. Electrochemical impedance spectroscopy measurements

A Volta-lab system instrument and a lock-in-amplifier connected to a personal computer were used to perform the electrochemical impedance spectroscopy experiments. The data analysis software was supplied with the instrument. The parameters for all impedance experiments were; frequency range of 0.1 Hz and 100 kHz and an excitation signal of 10 mV. The measurements were carried out under at certain potential values selected from the studied cyclic voltammograms.

### 2.3. Preparation of modified electrodes

CP was prepared by mixing graphite powder (0.5 g) with paraffin oil (0.3 mL) in a glassy mortar as reported earlier [26].  $\text{NdFeO}_3$  was prepared via microwave assisted-citrate method [26]. CP in-situ decorated with  $\text{NdFeO}_3$  perovskite was prepared by mixing different amounts of graphite powder (95, 90, 85, 80 and 75 %) with  $\text{NdFeO}_3$  (5, 10, 15, 20 and 25 %) to obtain 100 % total percent of the modified graphite. Then 250  $\mu\text{L}$  paraffin oil was mixed with 1 g of the modified graphite till a homogenous paste is obtained. The modified CP in this case was recognized as NFPCP.

The optimized percentage of  $\text{NdFeO}_3$  perovskite was further mixed with 2-chloro-1,3-dimethylimidazolium hexafluorophosphate ionic liquid crystal (ILC). 25 %  $\text{NdFeO}_3$  was further mixed with different amounts of graphite powder (70, 65, 60, 55 and 50 %) and ILC (5, 10, 15, 20 and 25 %) to obtain 100 % total percent of the modified graphite. Then 250  $\mu\text{L}$  paraffin oil was mixed with 1 g of the modified graphite till a homogenous paste is obtained.  $\text{NdFeO}_3/\text{ILC}$  modified CP in this case was recognized as NFILCCP.

The previously prepared electrodes CP, NFPCP and NFILCCP were utilized to examine the electrochemistry of 1  $\text{mmol L}^{-1}$  HQ and CC, each prepared in 0.1  $\text{mol L}^{-1}$  PBS/pH 7.0 in the presence of 100  $\mu\text{L}$  of 0.1  $\text{mol L}^{-1}$  SDS. The resulting electrodes were recognized as CP-SDS, NFPCP-SDS and NFILCCP-SDS, respectively.

Moreover, two other ionic liquids; 1-butyl-4-methylpyridinium tetrafluoroborate (IL1) and 1-hexyl-3-methylimidazolium tetrafluoroborate (IL2), were prepared by mixing ionic liquids with graphite powder with a ratio of 1% (w/w) using 250  $\mu\text{L}$  paraffin oil. Then 75% of ILs modified graphite was mixed with 25%  $\text{NdFeO}_3$ . The resulting electrodes were recognized as NFIL1CP and NFIL2CP, respectively. The electrodes were recognized as NFIL1CP-SDS and NFIL2CP-SDS, respectively in the presence of 100  $\mu\text{L}$  of 0.1  $\text{mol L}^{-1}$  SDS.

### 2.4. Optimization of $\text{NdFeO}_3$ and ILC in the CP

To achieve the highest electrochemical response toward the studied compounds, it is crucial to optimize the weight % of  $\text{NdFeO}_3$  perovskite and ILC inside the CP. The relation between the anodic peak current of 1  $\text{mmol L}^{-1}$  CC/0.1  $\text{mol L}^{-1}$  PBS/pH 7.0 and the weight % of  $\text{NdFeO}_3$  inside CP was studied. The highest current response of CC was obtained upon using 25 %  $\text{NdFeO}_3$  indicating that the optimum loading of  $\text{NdFeO}_3$  is 25 %, due to the increased number of active sites available for the reaction and increased active surface area. On the other hand, the relation between the anodic peak current of 1  $\text{mmol L}^{-1}$  CC/0.1  $\text{mol L}^{-1}$  PBS/pH 7.0 and the weight % of ILC (0 to 25 %) in presence of 25%  $\text{NdFeO}_3$  inside CP indicated that optimum % of ILC was 20 %. A slight increase in the current response and an obvious shift in the oxidation potential were observed upon any further increase in the ILC loading (> 20%). So, the optimum loading of ILC is 20 % (Figures not shown).

### 2.5. Real sample analysis

It is crucial to examine the real applicability of the studied method for simultaneous determination of HQ and CC in local tap water without any pretreatment steps. The local tap water

sample was used to prepare a stock solution of HQ and CC then standard additions were carried out from the stock solution in 10 mL of 0.1 mol L<sup>-1</sup> PBS/pH 7.0.

### 3. RESULTS AND DISCUSSION

#### 3.1. Morphology study

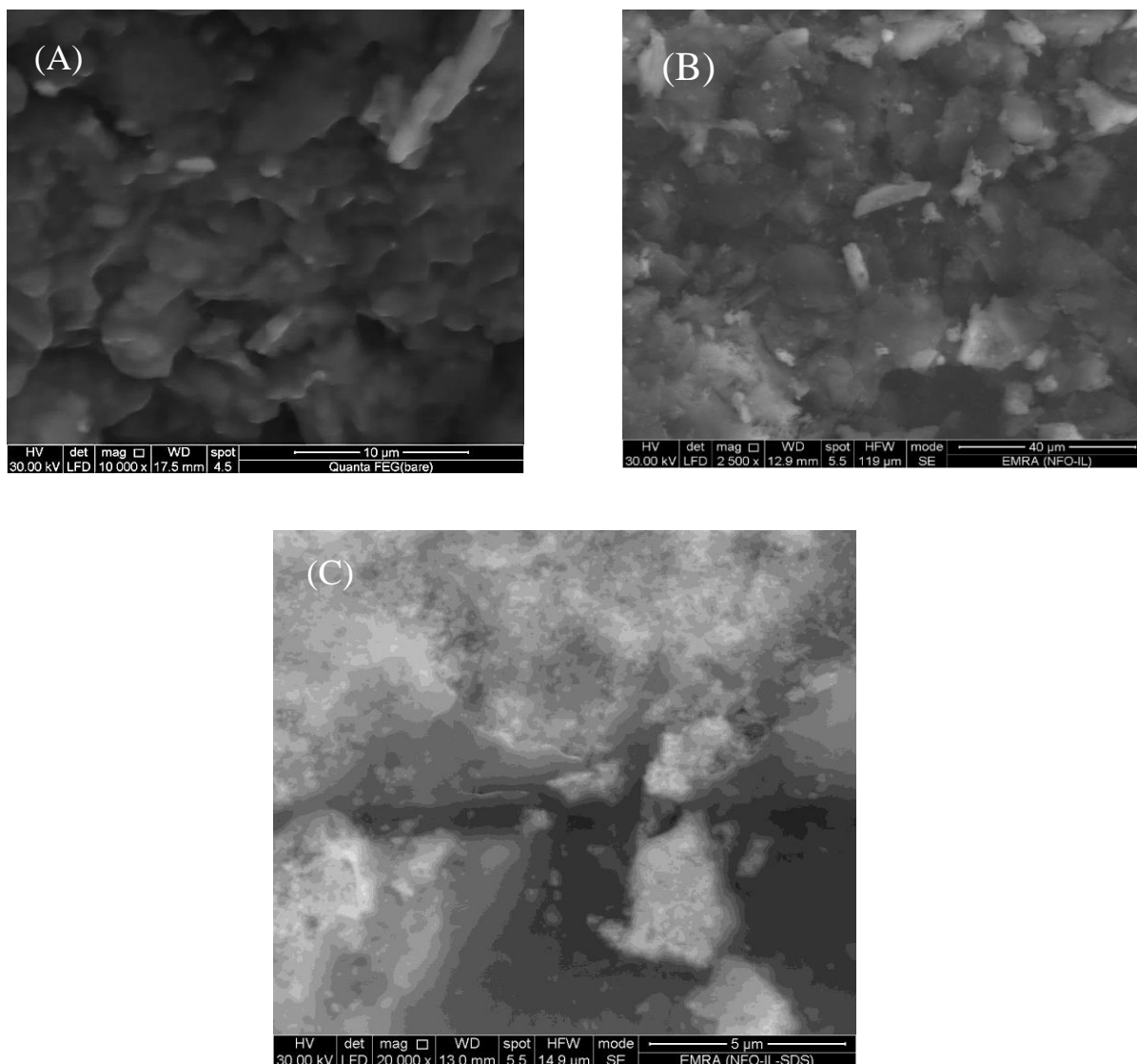


**Figure 1.** SEM of CP (A), NFILCCP (B) and NFILCCP-SDS (C).

Scanning electron microscopy has been used to investigate the morphology of the different electrodes surfaces. Figure 1 (A, B, C) shows the SEM of CP, NFILCCP and NFILCCP-SDS surfaces, respectively. The SEM of CP showed separated irregular graphite flakes (Figure 1(A)). A compact and blurry structure of NFILCCP was obtained upon modification of CP with NdFeO<sub>3</sub> and ILC modifiers (Figure 1(B)). The moderate viscosity and good conductivity of the ILC facilitated its distribution into the voids between the graphite flakes and enhanced its dispersion with the graphite powder and

NdFeO<sub>3</sub> in the paste. ILC proved to be excellent binder and ionic transportation channel between graphite flakes resulting in more conductive surface. Furthermore, spontaneous orientation of the ILC may induce NdFeO<sub>3</sub> inside the paste to form ordered molecularly packed microstructures, resulting in enhanced conductivity of the proposed composite [26]. The SEM of NFILCCP-SDS showed spongy films assembled on the surface of NFILCCP, enhancing the accumulation of analytes at the electrode surface (Figure 1(C)).

### 3.2. Electrochemical behavior of HQ and CC at different modified electrodes

In-situ modification of CP with NdFeO<sub>3</sub> nano-perovskite and ILC in presence of SDS resulted in enhanced electrochemical responses toward HQ and CC isomers. To demonstrate the electro-catalytic activity of the proposed composite, it is important to investigate the electrochemical responses of HQ and CC at different electrodes. The electrochemical responses of 1 mmol L<sup>-1</sup> HQ and 1 mmol L<sup>-1</sup> CC, each prepared in 0.1 mol L<sup>-1</sup> PBS/pH 7.0 are recorded at different working electrodes (bare CP, ILCCP, NFCP, NFILCCP and NFILCCP-SDS) as shown in Figure 2 (A, B), respectively.

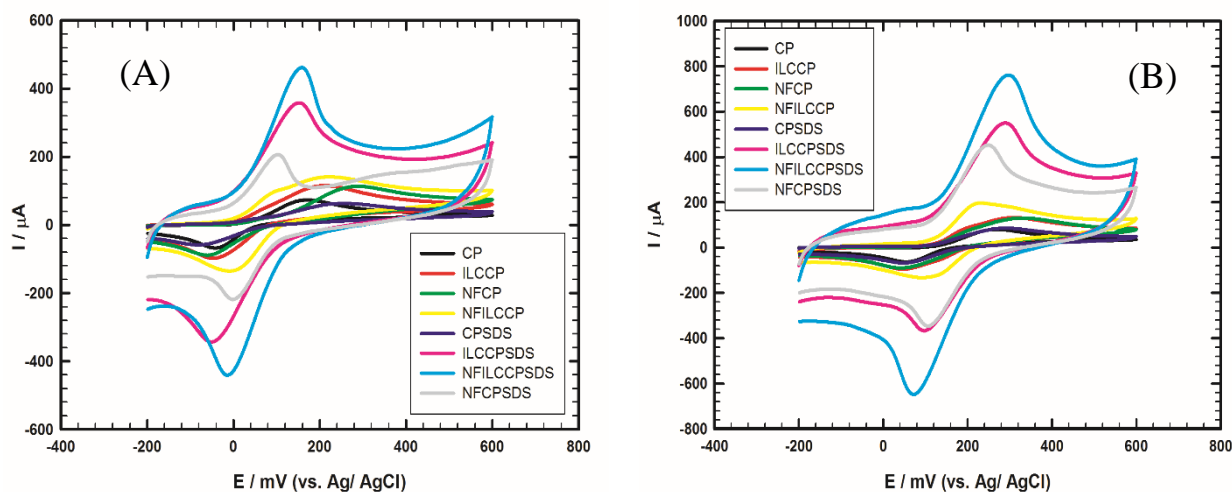


**Figure 2.** Cyclic voltammograms of (A) 1 mmol L<sup>-1</sup> of HQ/0.1 mol L<sup>-1</sup> PBS/pH 7.0, and (B) 1 mmol L<sup>-1</sup> of CC/0.1 mol L<sup>-1</sup> PBS/pH 7.0 recorded at different working electrodes; CP, NFCP, ILCCP, NFILCCP, CP-SDS, NFCP-SDS, ILCCP-SDS and NFILCCP-SDS, scan rate 50 mV s<sup>-1</sup>.

The anodic and cathodic peak current, anodic and cathodic peak potential and potential peak separation values are summarized in Table 1 for HQ and CC. Modification of CP with NdFeO<sub>3</sub> nano-perovskite and ILC resulted in a slight increase in the current responses of HQ and CC. Upon the addition of SDS, further noticeable increase in the anodic and cathodic peak current values in both HQ and CC was observed compared to the modified electrodes in absence of SDS. At NFILCCP-SDS, higher current responses toward electro-oxidation of both HQ and CC were obtained compared to other studied electrodes in presence of SDS (CP-SDS, NFCP-SDS, ILCCP-SDS) confirming the electro-catalytic activity of the proposed sensor (Table 1). The characteristic features of the proposed

sensor components are: high catalytic properties of  $\text{NdFeO}_3$  perovskite, high polarizability and excellent ionic conductivity of ILC. The  $\text{NdFeO}_3$  orthorhombic crystals are covered and separated with ILC conductive shell, resulting in enhanced conductivity, larger surface area and increase in the number of active sites available for the electrochemical reaction [26]. Furthermore, the SDS played a main role in enhancing the preconcentration/accumulation of HQ and CC at the conductive NFILCCP modified surface that in turn is reflected on the current signals. A synergistic role was realized by the coexistence of  $\text{NdFeO}_3$  perovskite, ILC and SDS resulting in enhanced electron transfer kinetics of HQ and CC at the proposed surface.

**Table 1.** Summary of CV results obtained at different electrodes for  $1 \text{ mmol L}^{-1}$  HQ and  $1 \text{ mmol L}^{-1}$  CC, each prepared in  $0.1 \text{ mol L}^{-1}$  PBS/pH 7.0.

Electrode	HQ						CC					
	$I_{pa}$ $\mu\text{A}$	$I_{pc}$ $\mu\text{A}$	$E_{pa}$ $\text{mV}$	$E_{pc}$ $\text{mV}$	$\Delta E$ $\text{mV}$	$D \times 10^{-6}$ $\text{cm}^2 \text{ s}^{-1}$	$I_{pa}$ $\mu\text{A}$	$I_{pc}$ $\mu\text{A}$	$E_{pa}$ $\text{mV}$	$E_{pc}$ $\text{mV}$	$\Delta E$ $\text{mV}$	$D \times 10^{-6}$ $\text{cm}^2 \text{ s}^{-1}$
CP	72.80	82.98	170	-43	213	1.94	80.80	79.00	270	54	216	2.39
ILCCP	114.9	112.7	210	-48	258	4.84	133.0	109.0	291	31	260	6.48
NFCP	112.8	76.48	287	-60	347	4.66	127.5	102.0	328	41	287	5.96
NFILCCP	125.4	153.6	223	-9	232	5.76	172.2	145.4	229	90	139	10.9
CP-SDS	54.00	58.47	253	-83	336	1.07	80.60	74.20	290	45	245	2.38
ILCCP-SDS	260.3	306.4	153	-51	204	24.8	427.7	308.3	289	98	191	67.05
NFCP-SDS	148.9	186.3	103	-1	104	8.13	338.2	308.9	248	107	141	41.93
<b>NFILCCP-SDS</b>	<b>355.5</b>	<b>401.5</b>	<b>158</b>	<b>-13</b>	<b>171</b>	<b>46.3</b>	<b>550.7</b>	<b>560.9</b>	<b>297</b>	<b>72</b>	<b>225</b>	<b>111.2</b>

### 3.3. Electrochemical behavior of ILC based electrode versus ILs

The catalytic activity of the proposed composite is affected by the type of ionic liquid used. The electrochemistry of  $1 \text{ mmol L}^{-1}$  HQ and  $1 \text{ mmol L}^{-1}$  CC, each prepared in  $0.1 \text{ mol L}^{-1}$  PBS/pH 7.0 was studied at NFILCCP-SDS, NFIL1CP-SDS and NFIL2CP-SDS, respectively (Figure not shown). The anodic peaks of HQ and CC were more resolved with enhanced current responses at NFILCCP-SDS compared to other electrodes. This result strongly proved the role of ILC in increasing the conductivity of the proposed composite. ILC with imidazolium cations showed good characteristics of chemical and electrochemical stability, low melting point and anisotropic conductivity resulting in highly conductive surface for further improved electrochemical oxidation of HQ and CC.

### 3.4. Effect of operational parameters

#### 3.4.1. Scan rate

It is very important to study the effect of applying different scan rates on the electrochemical responses of NFILCCP-SDS toward HQ and CC analytes. Figure 3 (A, B) shows the electrochemistry of 1 mmol L<sup>-1</sup> HQ and 1 mmol L<sup>-1</sup> CC, each prepared in 0.1 mol L<sup>-1</sup> PBS/pH 7.0 at NFILCCP-SDS at different scan rates from 10 to 100 mV s<sup>-1</sup>, respectively. Upon increasing the scan rate, the anodic peak current of each analyte increased and oxidation potential was shifted to more positive value. This indicated that the electrochemical oxidation of HQ and CC at NFILCCP-SDS is a quasi-reversible process. Inset of Figure 3 (A, B) shows the relations between the anodic and cathodic peak current values and the square root of the scan rate from 10 to 100 mV s<sup>-1</sup> for HQ and CC, respectively. Linear relations were obtained in HQ and CC indicating that the electrochemical oxidation of HQ and CC was under diffusion control [1, 3, 4, 6].

The linear relations for HQ were obtained and fitted to equations 1, 2:

$$I_{pa} \text{ (A)} = 2.076 \times 10^{-3} V^{1/2} \text{ (V/s)}^{1/2} - 1.145 \times 10^{-4} \quad (1)$$

$$R^2 = 0.999$$

$$I_{pc} \text{ (A)} = -2.592 \times 10^{-3} V^{1/2} \text{ (V/s)}^{1/2} + 1.371 \times 10^{-4} \quad (2)$$

$$R^2 = 0.998$$

And the linear relations for CC were obtained and fitted to equations 3, 4:

$$I_{pa} \text{ (A)} = 2.030 \times 10^{-3} V^{1/2} \text{ (V/s)}^{1/2} - 1.354 \times 10^{-5} \quad (3)$$

$$R^2 = 0.997$$

$$I_{pc} \text{ (A)} = -2.569 \times 10^{-3} V^{1/2} \text{ (V/s)}^{1/2} + 1.010 \times 10^{-4} \quad (4)$$

$$R^2 = 0.999$$

Randles-Sevcik equation (eqn. 5) for a quasi-reversible process was used to calculate the apparent diffusion coefficients ( $D_{app}$ , cm<sup>2</sup>/s) of HQ and CC at different modified electrodes to confirm the difference in their electro-catalytic activities.

$$I_p^{quasi} = \pm(2.65 \times 10^5) n^{3/2} ACv^{1/2} D^{1/2} \quad (5)$$

Where A is the geometric area (cm<sup>2</sup>), n is the total number of electrons transferred per molecule in the electrochemical process,  $D_{app}$  is the apparent diffusion coefficient (cm<sup>2</sup>/s), C is the analyte concentration (mol/cm<sup>3</sup>) and v is the scan rate (V/s) at the absolute temperature (T= 298 k) [38]. The values of  $D_{app}$  for HQ and CC at different modified electrodes are summarized in Table 1 showing the highest values are obtained at NFILCCP-SDS for both HQ and CC. Increasing in the values of  $D_{app}$  upon modification confirming the electro-catalytic activity of the proposed surface.

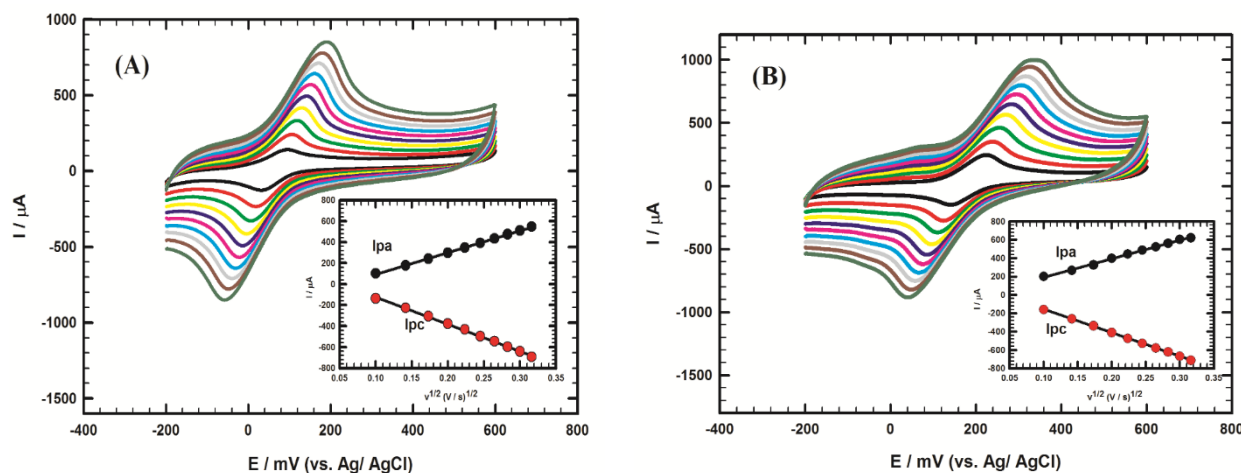
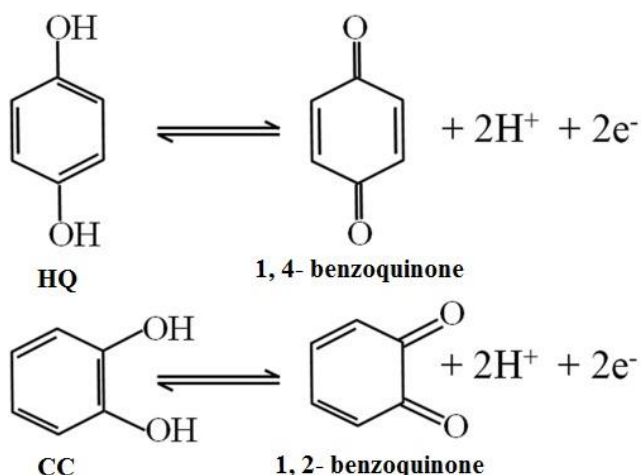


**Figure 3.** Cyclic voltammograms of (A)  $1 \text{ mmol L}^{-1}$  of HQ/ $0.1 \text{ mol L}^{-1}$  PBS/pH 7.0 and (B)  $1 \text{ mmol L}^{-1}$  of CC/ $0.1 \text{ mol L}^{-1}$  PBS/pH 7.0 recorded at NFILCCP-SDS at different scan rate values from 10 to 100 mV/s. Insets: Plots of the anodic and cathodic peak current values of HQ and CC as a function of the square root of scan rate.

### 3.4.2. pH of the supporting electrolyte

The effect of the pH on the electrochemical oxidation responses for of  $1 \text{ mmol L}^{-1}$  HQ and  $1 \text{ mmol L}^{-1}$  CC, each prepared in  $0.1 \text{ mol L}^{-1}$  PBS of different pH values (2-9) at NFILCCP-SDS was investigated (Figures not shown). Upon increasing the pH of the supporting electrolyte, the anodic peak potential of each analyte was shifted to less positive value indicating that protonation and deprotonation are taking part in the electrochemical process.



**Scheme 1.** Electrochemical oxidation of HQ and CC.

Figure 4 (A, B) shows the relations between the anodic peak potential values of HQ and CC at NFILCCP-SDS and the pH respectively. Linear relations were obtained and fitted to (eqns. 6 and 7) for HQ and CC, respectively.

$$E_{pa} \text{ (V)} = 0.544 - 0.0515 \text{ pH} \quad (6)$$

$$R^2 = 0.977$$

$$E_{pa} \text{ (V)} = 0.732 - 0.0543 \text{ pH} \quad (7)$$

$$R^2 = 0.913$$

The slopes of these relations are ( $-0.0515 \text{ V/pH}$ ) and ( $-0.0543 \text{ V/pH}$ ) for HQ and CC, respectively which is nearly the same as the Nernstian slope. The results ascertain that the number of protons and electrons involved in the electron transfer step is the same ( $2e^-/2H^+$ ) [1, 4, 6]. Scheme 1 indicated the electrochemical oxidation of HQ and CC.

Insets of Figure 4 (A, B) show the relations between the anodic peak current values of HQ and CC versus the pH, respectively. The anodic peak current of HQ reached its maximum value at pH 7 then decreased again. While for CC, the anodic peak current of CC increased until became constant with increasing the pH value. In the present study, pH 7.0 was chosen for subsequent measurements.

### 3.5. Performance characteristics of the proposed sensor

#### 3.5.1. Stability studies

Stability of the electrochemical response is an important characteristic of any sensor affecting its performance and impact toward the determination of different analytes. The stability of NFILCCP-SDS sensor was investigated via repeated cycle stability up to 25 cycles in  $1 \text{ mmol L}^{-1} \text{ HQ}/0.1 \text{ mol L}^{-1} \text{ PBS/pH 7.0}$  and  $1 \text{ mmol L}^{-1} \text{ CC}/0.1 \text{ mol L}^{-1} \text{ PBS/pH 7.0}$ . Stable response without obvious decrease in the anodic peak current or shift in the anodic peak potential was obtained in each analyte indicating the resistance of the suggested surface from fouling by the oxidation products (Figures not shown).

The long-term stability of NFILCCP-SDS up to one month of storage was studied in  $1 \text{ mmol L}^{-1} \text{ HQ}/0.1 \text{ mol L}^{-1} \text{ PBS/pH 7.0}$  and  $1 \text{ mmol L}^{-1} \text{ CC}/0.1 \text{ mol L}^{-1} \text{ PBS/pH 7.0}$ . The electrodes were stored in open air at room temperature. There is no decrease in the current responses after one month of storage in both cases indicating excellent long-term stability of the electrochemical signals of HQ and CC at the suggested surface.

Furthermore NFILCCP-SDS sensor was used to investigate the electrochemical responses toward each of  $1 \text{ mmol L}^{-1} \text{ HQ}/0.1 \text{ mol L}^{-1} \text{ PBS/pH 7.0}$  and  $1 \text{ mmol L}^{-1} \text{ CC}/0.1 \text{ mol L}^{-1} \text{ PBS/pH 7.0}$ ; for three times using the same electrode tested in the same solution. The relative standard deviation values were 0.736 % and 0.699 % for HQ and CC, respectively. Three different NFILCCP-SDS electrodes prepared by the same way tested in the same solution were utilized to perform three independent measurements in each of  $1 \text{ mmol L}^{-1} \text{ HQ}/0.1 \text{ mol L}^{-1} \text{ PBS/pH 7.0}$  and  $1 \text{ mmol L}^{-1} \text{ CC}/0.1 \text{ mol L}^{-1} \text{ PBS/pH 7.0}$  to confirm the reproducibility of the proposed surface. The relative standard deviation values were 0.327 % and 0.466 % for HQ and CC, respectively.

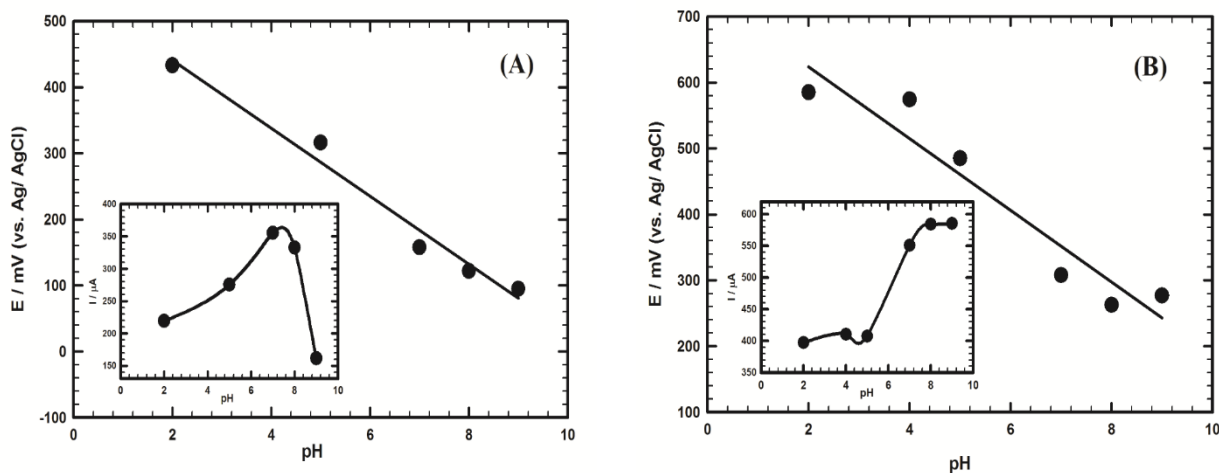


**Figure 4.** Plots of the anodic peak potential of 1 mmol L<sup>-1</sup> of HQ/0.1 mol L<sup>-1</sup> PBS (A) and 1 mmol L<sup>-1</sup> of CC/0.1 mol L<sup>-1</sup> PBS (B) versus the pH values in the range of (2-9). Insets: The relation between the current values of each analyte versus the pH values.

### 3.5.2. Robustness`

The stability of the current response was examined upon the influence of minor variation in the experimental parameters. The parameters under study were ILC % ( $20\% \pm 0.1$ ), time before measurement (2 minutes  $\pm 20$  s) and pH change ( $7.0 \pm 0.2$ ). The relative standard deviation values were 0.750 %, 0.460 % and 0.742 % for HQ and 0.786 %, 0.442 % and 1.08 % for CC, respectively. These values confirm the robustness and the credibility of the present method during the measurements.

### 3.5.3. Precision

Analyses of the same concentration in a single run and in three separate runs three times were achieved for every compound to examine the intra-day and inter-day precisions, respectively. The relative standard deviation values were 0.674 % and 1.06 % for HQ and 0.209 % and 0.584 % for CC, respectively. These values confirm the convenience of the applied method for quality control analysis of HQ and CC with good precision.

### 3.6. Selectivity and Interference studies

Since the oxidation peak potentials for HQ and CC were close to each other, so the interference studies were investigated when they coexist in the same solution. Figure 5 shows the square wave voltammogram (SWV) of tertiary mixture of equimolar concentration of 1 mmol L<sup>-1</sup> of HQ, CC and RC prepared in 0.1 mol L<sup>-1</sup> PBS/pH 7.0 at NFILCCP-SDS. Three well-defined oxidation peaks were obtained with good potential peaks separation of 130 mV and 340 mV between HQ /CC and CC /RC,

respectively demonstrating the ability of the proposed surface to simultaneously detect HQ, CC and RC.

Besides, the interference of various cations and anions existing in water samples like  $\text{Na}^+$ ,  $\text{Mg}^{2+}$ ,  $\text{Pb}^{2+}$ ,  $\text{Cd}^{2+}$ ,  $\text{Mn}^{2+}$ ,  $\text{K}^+$ ,  $\text{Ca}^{2+}$ ,  $\text{Cu}^{2+}$  and  $\text{Cl}^-$  with 100-folds concentration has been investigated on the simultaneous determination of HQ and CC at NFILCCP-SDS. It was found that no significant variation of the anodic peak current values of HQ and CC (less than 5%) due to the presence of these interfering ions with no shift in the oxidation potential values. This indicated the good selectivity and anti-interference capability of the proposed surface toward the simultaneous detection of structurally similar compounds in the presence of interfering ions.

### 3.7. Analytical performance

#### 3.7.1. Determination of HQ and CC at NFILCCP-SDS

The sensitivity of NFILCCP-SDS toward HQ and CC determination has been studied using square wave voltammetry (SWV) technique. Figure 6A (inset) shows the SWVs of the determination of HQ in the concentration range of 30 to 260  $\mu\text{mol L}^{-1}$  in the presence of 200  $\mu\text{mol L}^{-1}$  CC at NFILCCP-SDS. The calibration curve of HQ in the presence of 200  $\mu\text{mol L}^{-1}$  CC is shown in Figure 6A. The linear regression equation of HQ could be fitted to (eqn. 8):

$$I_p (\mu\text{A}) = 0.3345 C (\mu\text{mol L}^{-1}) + (-15.57) \quad (8)$$

$$R^2 = 0.982$$

The sensitivity of the proposed sensor toward HQ in the presence of 200  $\mu\text{mol L}^{-1}$  CC is 0.3345  $\mu\text{A}/\mu\text{mol L}^{-1}$ , detection limit is 0.120  $\mu\text{mol L}^{-1}$  and quantification limit is 0.402  $\mu\text{mol L}^{-1}$ .

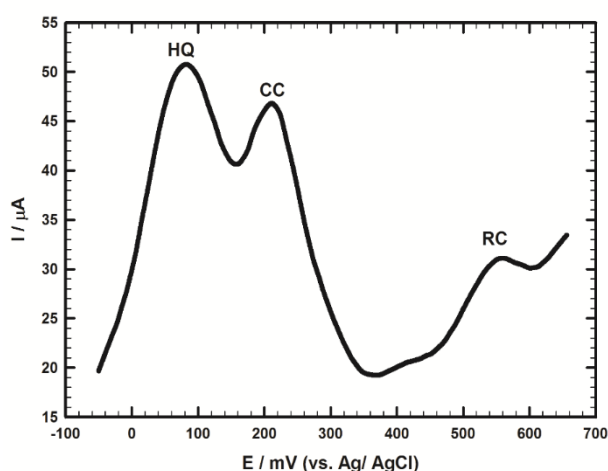


**Figure 5.** SWV for tertiary mixture of equimolar concentration of 1  $\text{mmol L}^{-1}$  of HQ, CC and RC prepared in 0.1  $\text{mol L}^{-1}$  PBS/pH 7.0 at NFILCCP-SDS.

On the other hand, the SWVs of the determination of CC in the concentration range of 30 to 260  $\mu\text{mol L}^{-1}$  in the presence of 200  $\mu\text{mol L}^{-1}$  HQ at NFILCCP-SDS are shown in the inset of Figure

6B. The calibration curve of CC in the presence of 200  $\mu\text{mol L}^{-1}$  HQ is shown in Figure 6B. The linear regression equation of CC could be fitted to (eqn. 9):

$$I_p (\mu\text{A}) = 0.2696 C (\mu\text{mol L}^{-1}) + (-10.34) \quad (9)$$

$$R^2 = 0.975$$

The sensitivity of the proposed sensor toward CC in the presence of 200  $\mu\text{mol L}^{-1}$  HQ is 0.2696  $\mu\text{A}/\mu\text{mol L}^{-1}$ , detection limit is 0.150  $\mu\text{mol L}^{-1}$  and quantification limit is 0.498  $\mu\text{mol L}^{-1}$ .

Moreover, the SWVs of the simultaneous determination of HQ and CC in the concentration range of 10 to 180  $\mu\text{mol L}^{-1}$  at NFILCCP-SDS are shown in the inset of Figure 6C. The calibration curves of HQ and CC in the concentration range of 10 to 180  $\mu\text{mol L}^{-1}$  are shown in Figure 6C and the inset, respectively.

The linear regression equation of HQ in the concentration range of 10 to 180  $\mu\text{mol L}^{-1}$  could be fitted to (eqn. 10):

$$I_p (\mu\text{A}) = 0.3429 C (\mu\text{mol L}^{-1}) + (0.3095) \quad (10)$$

$$R^2 = 0.989$$

The sensitivity is 0.3429  $\mu\text{A}/\mu\text{mol L}^{-1}$ , detection limit is 0.118  $\mu\text{mol L}^{-1}$  and quantification limit is 0.392  $\mu\text{mol L}^{-1}$ .

And the linear regression equation of CC in the concentration range of 10 to 180  $\mu\text{mol L}^{-1}$  could be fitted to (eqn. 11):

$$I_p (\mu\text{A}) = 0.1600 C (\mu\text{mol L}^{-1}) + (-0.1105) \quad (11)$$

$$R^2 = 0.989$$

The sensitivity is 0.1600  $\mu\text{A}/\mu\text{mol L}^{-1}$ , detection limit is 0.252  $\mu\text{mol L}^{-1}$  and quantification limit is 0.840  $\mu\text{mol L}^{-1}$ .

The detection limit (DL) and quantification limit (QL) were calculated from the equations (eqns. 12, 13), respectively:

$$DL = 3 s / b \quad (12)$$

$$QL = 10 s / b \quad (13)$$

Where  $s$  is the standard deviation and  $b$  is the slope of the calibration curve.

Table 2 shows comparison for simultaneous determination of HQ and CC at different electrodes based on literature showing a lower detection limit at the proposed sensor compared to other electrodes mentioned in literature. This comparison revealed that the synergistic presence of  $\text{NdFeO}_3$ , ILC and SDS, facilitated the electron transfer rate and improved the detection limit values of HQ and CC at the proposed surface.

### 3.7.2. Determination of HQ and CC in tap water samples

The application of the simultaneous determination of HQ and CC in tap water sample was examined to evaluate the practicability of NFILCCP-SDS in real sample analysis. The recovery results were in the acceptable range of 98.6 % to 103.1 % and 99.04 % to 100.7 % for HQ and CC, respectively as shown in Table 3. This result ensured that this method is applicable for the simultaneous determination of HQ and CC in real samples with good accuracy and satisfied results.

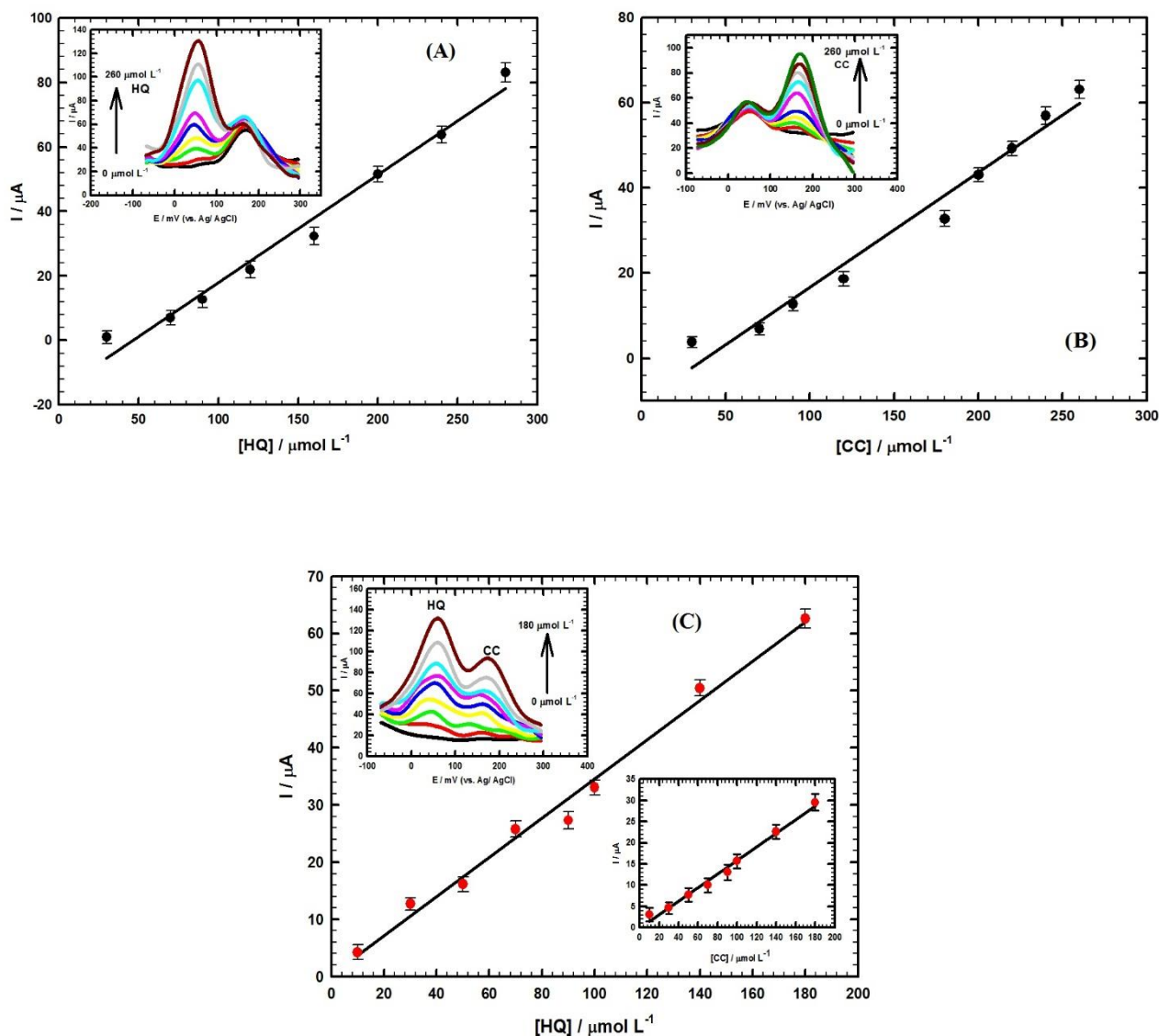


**Figure 6.** (A) Calibration curve of HQ in the concentration range of 30-260 μmol L<sup>-1</sup> in the presence of 200 μmol L<sup>-1</sup> CC at NFILCCP-SDS. Inset: SWVs of HQ in the concentration range of 30-260 μmol L<sup>-1</sup> in the presence of 200 μmol L<sup>-1</sup> CC at NFILCCP-SDS. (B) Calibration curve of CC in the concentration range of 30-260 μmol L<sup>-1</sup> in the presence of 200 μmol L<sup>-1</sup> HQ at NFILCCP-SDS. Inset: SWVs of CC in the concentration range of 30-260 μmol L<sup>-1</sup> in the presence of 200 μmol L<sup>-1</sup> HQ at NFILCCP-SDS. (C) Calibration curve of HQ in the concentration range of 10-180 μmol L<sup>-1</sup> at NFILCCP-SDS. Insets: SWVs of simultaneous determination of HQ and CC in the concentration range of 10-180 μmol L<sup>-1</sup> at NFILCCP-SDS and calibration curve of CC in the concentration range of 10-180 μmol L<sup>-1</sup> at NFILCCP-SDS.

**Table 2.** Comparison of NFILCCP-SDS electrode with different modified electrodes mentioned in literature for simultaneous determination of HQ and CC.

Electrode	Linear dynamic range / $\mu\text{mol L}^{-1}$		Detection limit / $\mu\text{mol L}^{-1}$	
	HQ	CC	HQ	CC
Copper(II) complex and single-walled carbon nanotubes modified glassy carbon electrode [3]	5–370	5–215	1.46	3.50
Activated graphene oxide modified screen printed electrode [5]	1–312	1–350	0.270	0.182
Glassy carbon electrode modified with penicillamine [6]	15–115	25–175	1	0.6
Cu-based metal organic frame and graphene oxide [7]	0.1-476	0.1-566	0.1	0.1
Carbon dots/ reduced graphene oxide composite on the glassy carbon electrode [8]	0.5-1000	1.0-950	0.17	0.28
Graphene–chitosan composite film modified glassy carbon electrode [11]	1-300	1-400	0.75	0.75
Cobalt ferrite modified carbon paste electrode [15]	1-120	1-85	0.3	0.15
Poly(3-thiophenemalonic Acid) modified glassy carbon electrode [18]	7.81-500	3.91-500	7.81	3.91
Poly(4-vinylphenylboronic acid) functionalized polypyrrole/graphene oxide nanosheets [20]	4-22	7-16	0.53	0.96
Graphene screen-printed electrode [39]	1-35	1-38.1	2.7	1.7
Gold nanoparticles mesoporous silica modified carbon paste electrode [40]	10-1000	30-1000	1.2	1.1
Glassy carbon electrode modified with carboxy-functionalized carbon nanotubes in a chitosan matrix and decorated with gold nanoparticles [41]	0.5-1500	5-900	0.17	0.89
Poly(niacinamide) modified glassy carbon electrode [42]	10-160	10-120	0.31	0.24
Electrochemically polymerized neutral red on the surface of carbon paste electrode [43]	20-120	10-100	4.97	6.46
Three-dimensionally ordered macroporous polycysteine film modified electrode [44]	9-700	3-700	2	0.5
A disposable pencil graphite electrode modified with cobalt-phthalocyanine [45]	0.5-100	0.5-100	0.338	0.34
Au-Pd nanoflower/reduced graphene oxide nanocomposite [46]	1.6-440	2.5-460	0.5	0.85

Flower-like Pd-graphene composites [47]	10-1000	10-1000	1.25	1
Covalent layer-by-layer self-assembly of carboxylated- multiwall carbon nanotubes [48]	10-120	5-80	2.3	1
Reduced graphene oxide and multiwall carbon nanotubes hybrid materials [49]	8-391	5.5-5400	2.6	1.8
Poly (malachite green) coated multiwalled carbon nanotube film [50]	10-480	30-1190	1.6	5.8
<b>NFILCCP-SDS [This work]</b>	10-180	10-180	0.118	0.252

**Table 3.** Evaluation of the accuracy and precision of the proposed method for the determination of HQ and CC in tap water sample.

Sample.	added $\mu\text{mol L}^{-1}$		found $\mu\text{mol L}^{-1}$		Recovery %	
	HQ	CC	HQ	CC	HQ	CC
<b>1</b>	50	50	49.3	50.35	98.6	100.7
<b>2</b>	70	70	72.17	69.33	103.1	99.04
<b>3</b>	180	180	179.86	179.86	99.92	99.92
<b>4</b>	320	320	319.74	321.31	99.92	100.41

### 3.8. Electrochemical Impedance Spectroscopy

Electrochemical impedance spectroscopy can successfully be employed for characterization of different electrochemical systems and to elucidate the electrode/electrolyte processes. A brief image of the surface modification and its corresponding variation in the charge transfer kinetics and capacitive components of the system can be presented by the aid of EIS. The impedance spectra in the form of Nyquist plots for CP and NFILCCP-SDS electrodes in HQ and CC are shown in Figure 7A and 7C, respectively. EIS experiments were applied in  $1 \text{ mmol L}^{-1}$  HQ/ $0.1 \text{ mol L}^{-1}$  PBS/pH 7.0 and CC/ $0.1 \text{ mol L}^{-1}$  PBS/pH 7.0 at an AC frequency (0.1 Hz to 100 kHz) at the corresponding oxidation potential values of analytes at the CP and NFILCCP-SDS electrodes, respectively. The Nyquist plots for CP in both cases of HQ and CC were identified by a semicircle part at higher frequency and a linear part at lower frequency. These parts are corresponding to electron-transfer limited and diffusion-limited processes, respectively. The semicircle diminished sharply, while a linear part only was obtained for NFILCCP-SDS in both analytes. These observations reflected that upon modification, the charge transfer resistance decreased reflecting the enhancement of the charge transfer rate owing to the interactive impact of the individual components of the proposed composite. Also, there is an obvious decrease in the values of the total impedance in the order of NFILCCP-SDS < CP at the same frequency value in both analytes (Figure 7A and C). A modified Randle's circuit is used to fit the corresponding EIS data for both analytes (Inset of Figure 7A). The fitting data using this circuit are represented as solid lines in EIS spectra and a good agreement was obtained between the experimental

and fitting data. The proposed process involved a combination of kinetic and diffusion controlled processes. So, the equivalent circuit contained:  $R_s$  (ohmic solution resistance),  $R_{ct}$  (charge transfer resistance),  $Y_{o1}$  (constant phase element owing to the roughness of the corresponding surfaces and reaction rates inhomogeneity at the surfaces) and  $W_{s1}$  (Warburg impedance due to diffusion of corresponding ions from the bulk of solution to surface of the electrode). Table 4 contains the fitting data for both compounds corresponding to Figure 7.

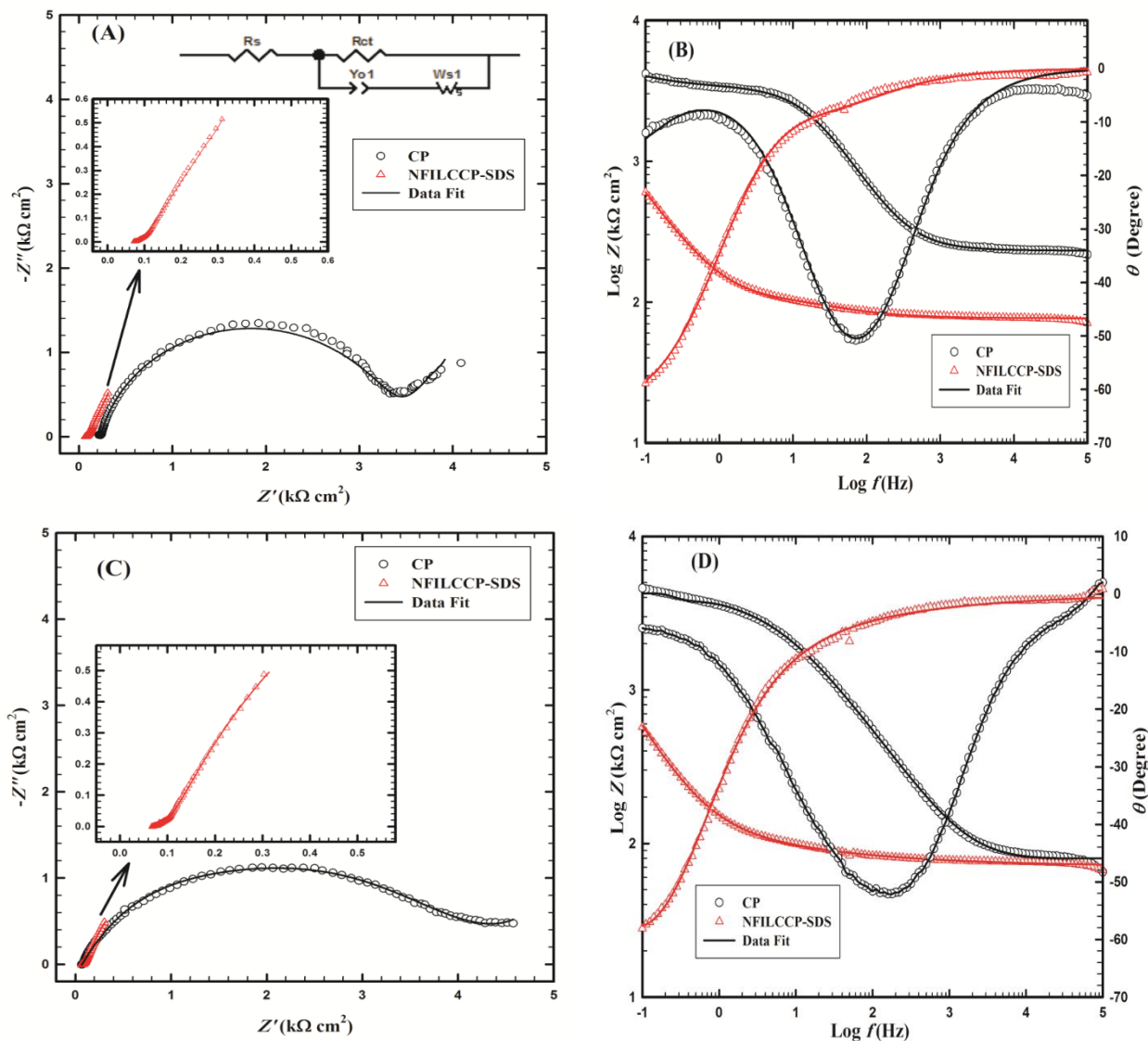


**Figure 7.** (A), (C) Typical impedance spectra presented in the form of the Nyquist plots for CP ( $\circ$ ) and NFILCCP-SDS ( $\Delta$ ) for HQ and CC, respectively. (Symbols and solid lines represent the experimental measurements and the computer fitting of impedance spectra, respectively). (Inset): Equivalent circuit used in the fit procedure of the impedance spectra. (B), (D) Bode plots for CP ( $\circ$ ) and NFILCCP-SDS ( $\Delta$ ) for HQ and CC, respectively.

There is a decrease in the values of  $R_{ct}$  and  $W_{s1}$  of NFILCCP-SDS upon modification compared to CP indicating the characteristic features of the proposed surface. In addition, an obvious increase in

$Y_{01}$  value of NFILCCP-SDS compared to CP with  $n \sim 1$  confirming the capacitive nature of the proposed composite. The impedance spectra in the form of Bode plots for CP and NFILCCP-SDS electrodes in HQ and CC are shown in Figure 7B and 7D, respectively. The total impedance values at relatively lower frequencies decreased in the order of NFILCCP-SDS < CP demonstrating a good agreement regarding total impedance between Nyquist and Bode plots. The total impedance at low frequency is corresponding to  $R_{ct}$  values with the expected order in Table 4 showing the lowest values for NFILCCP-SDS in both analytes. EIS values revealed the combined interaction between the components of the proposed composite resulting in enhancing kinetic and thermodynamic favoring routes.

**Table 4.** EIS fitting data corresponding to Figure 7 for HQ and CC.

	HQ		CC	
	CP	NFILCCP-SDS	CP	NFILCCP-SDS
$R_s$ ( $\Omega \text{ cm}^2$ )	232.1	76.85	82.75	71.19
$R_{ct}$ ( $\Omega \text{ cm}^2$ )	3158	1051	4214	1232
$W_{s1}$ ( $\Omega \text{ s}^{-1/2}$ )	4203	1321	3245	653.5
$Y_0$ ( $\text{F cm}^{-2}$ )	$6.123 \times 10^{-6}$	$1.217 \times 10^{-3}$	$9.225 \times 10^{-6}$	$1.280 \times 10^{-4}$
n	0.862	0.898	0.871	0.913

#### 4. CONCLUSIONS

In the present work, we utilized  $\text{NdFeO}_3/\text{ILC}$  as in-situ modifiers for carbon paste electrode for the simultaneous determination of HQ and CC in the presence of sodium dodecyl sulfate. The  $\text{NdFeO}_3/\text{ILC}$  modifiers increased the conductivity level and the surface area of the modified surface. Furthermore, SDS was used to enhance the current response and selectivity toward HQ and CC at NFILCCP electrode surface. Under the optimum conditions, the linear dynamic range for HQ and CC was 10 to 180  $\mu\text{mol L}^{-1}$  with limit of detections of 0.118  $\mu\text{mol L}^{-1}$  and 0.252  $\mu\text{mol L}^{-1}$ , respectively. The proposed composite showed a characteristic performance making it useful for determination of HQ and CC pollutants in environment and biological samples.

#### ACKNOWLEDGEMENT

The authors would like to acknowledge the financial support from Cairo University through the Vice President Office for Research Funds.

#### References

1. Q. Yu, Y. Liu, X. Liu, X. Zeng, S. Luo and W. Wei, *Electroanalysis*, 9 (2010) 1012.
2. H. Zhang, X. Bo and L. Guo, *Sens. Actuators, B*, 220 (2015) 919.
3. L.A. Alshahrani, X. Li, H. Luo, L. Yang, M. Wang, S. Yan, P. Liu, Y. Yang and Q. Li, *Sensors*, 14 (2014) 22274.
4. C. Wei, Q. Huang, S. Hu, H. Zhang, W. Zhang, Z. Wang, M. Zhu, P. Dai and L. Huang, *Electrochim. Acta*, 149 (2014) 237.

5. M. Velmurugan, N. Karikalan, S. Chen, Y. Cheng and C. Karuppiah, *J. Colloid Interface Sci.*, 500 (2017) 54.
6. L. Wang, P.F. Huang, J.Y. Bai, H.J. Wang, L.Y. Zhang and Y.Q. Zhao, *Microchim. Acta*, 158 (2007) 151.
7. Q. Chen, X. Li, X. Min, D. Cheng, J. Zhou, Y. Li, Z. Xie, P. Liu, W. Cai and C. Zhang, *J. Electroanal. Chem.*, 789 (2017) 114.
8. W. Zhang, J. Zheng, Z. Lin, L. Zhong, J. Shi, C. Wei, H. Zhang, A. Hao and S. Hu, *Anal. Methods*, 7 (2015) 6089.
9. P.S. Ganesh, B.E.K. Swamy and K.V. Harisha, *Anal. Bioanal. Electrochem.*, 9 (2017) 47.
10. L.A. Goular and L.H. Mascaro, *Electrochim. Acta*, 196 (2016) 48.
11. H. Yin, Q. Zhang, Y. Zhou, Q. Ma, T. Liu, L. Zhu and S. Ai, *Electrochim. Acta*, 56 (2011) 2748.
12. Z. Liu, Z. Wang, Y. Cao, Y. Jing and Y. Liu, *Sens. Actuators, B*, 157 (2011) 540.
13. W. Sun, Y. Wang, Y. Lu, A. Hu, F. Shi and Z. Sun, *Sens. Actuators, B*, 188 (2013) 564.
14. Q. Guo, M. Zhang, G. Zhou, L. Zhu, Y. Feng, H. Wang, B. Zhong and H. Hou, *J. Electroanal. Chem.*, 760 (2016) 15.
15. M. Lakic, A. Vukadinovic, K. Kalcher, A.S. Nikolic and D.M. Stankovic, *Talanta*, 161 (2016) 668.
16. H. Wei, X. Wu, G. Wen and Y. Qiao, *Molecules*, 21 (2016) 617.
17. S. Cui, L. Li, Y. Ding and J. Zhang, *J. Electroanal. Chem.*, 782 (2016) 225.
18. G. Xu, B. Tang, S. Jing and J. Tao, *Int. J. Electrochem. Sci.*, 10 (2015) 10659.
19. S. Palanisamy, C. Karuppiah, S. Chen, C. Yang and P. Periakaruppan, *Anal. Methods*, 6 (2014) 4271.
20. H. Mao, M. Liu, Z. Cao, C. Ji, Y. Sun, D. Liu, S. Wu, Y. Zhang and X. Song, *Appl. Surf. Sci.*, 420 (2017) 594.
21. M. Li, F. Ni, Y. Wang, S. Xu, D. Zhang, S. Chen and L. Wang, *Electroanalysis*, 21 (2009) 1521.
22. C. Bu, X. Liu, Y. Zhang, L. Li, X. Zhou and X. Lu, *Colloids Surf., B*, 88 (2011) 292.
23. N.F. Atta, A. Galal, S.M. Azab and A.H. Ibrahim, *J. Electrochem. Soc.*, 162 (2015) B9.
24. S. Tajik, M.A. Taher and H. Beitollahi, *Ionics*, 20 (2014) 1155.
25. P.S. Ganesh and B.E.K. Swamy, *J. Mol. Liq.*, 220 (2016) 208.
26. N.F. Atta, E.H. El-Ads and A. Galal, *J. Electrochem. Soc.*, 163 (2016) B325.
27. X. Wang, M. Wu, H. Li, Q. Wang, P. He and Y. Fang, *Sens. Actuators, B*, 192 (2014) 452.
28. X. Wang, Y. Cheng, Z. You, H. Sha, S. Gong, J. Liu and W. Sun, *Ionics*, 21 (2015) 877.
29. G. Li, T. Li, Y. Deng, Y. Cheng, F. Shi, W. Sun and Z. Sun, *J. Solid State Electrochem.*, 17 (2013) 2333.
30. N.F. Atta, M.H. Binsabt, S.H. Hassan and A. Galal, *Crystals*, 7 (2017) 27.
31. N.F. Atta, A. Galal and E.H. El-Ads, *Perovskite Nanomaterials – Synthesis, Characterization, and Applications*, InTech, 2016, pp. 107.
32. P.E. Marti and A. Baiker, *Catal. Lett.*, 26 (1994) 71.
33. S. Singh, A. Singh, B.C. Yadav and P.K. Dwivedi, *Sens. Actuators, B*, 177 (2013) 730.
34. C. Tongyun, S. Liming, L. Feng, Z. Weichang, Z. Qianfeng and C. Xiangfeng, *J. Rare Earth*, 30 (2012) 1138.
35. S. Chanda, S. Saha, A. Dutta and T.P. Sinha, *Mater. Res. Bull.*, 48 (2013) 1688.
36. S.A. Mir, M. Ikram and K. Asokan, *Optik*, 125 (2014) 6903.
37. N.F. Atta, M.H. Binsabt, E.H. El-Ads and A. Galal, *Turk. J. Chem.*, 41 (2017) 476.
38. D.A.C. Brownson and C.E. Banks, *Interpreting Electrochemistry*, Springer, London Heidelberg New York Dordrecht 2014, pp. 23.
39. M. Aragón, C. Ariño, À. Dago, J.M. Díaz-Cruz and M. Esteban, *Talanta*, 160 (2016) 138.
40. J. Tashkhourian, M. Daneshi, F. Nami-Ana, M. Behbahani and A. Bagheri, *J. Hazard. Mater.*, 318 (2016) 117.
41. Y. Shen, D. Rao, Q. Sheng and J. Zheng, *Microchim Acta*, 184 (2017) 3591.

42. A. Anil Kumar, B.E. Kumara Swamy, P.S. Ganesh, T. Shobha, Rani and G. Venkata Reddy, *J. Electroanal. Chem.*, 799 (2017) 505.
43. T.S. Sunil Kumar Naik and B.E. Kumara Swamy, *J. Electroanal. Chem.*, 804 (2017) 78.
44. J. Wang, Z. Shi, J. Jing, Y. Tan, S. Zhang and Dating Tian, *Russ. J. Electrochem.*, 52(3) (2016) 283.
45. M. Buleandra, A.A. Rabinca, I.A. Badea, A. Balan, I. Stamatina, C. Mihailciuc and A.A. Ciucu, *Microchim. Acta.*, 184(5) (2017) 1481.
46. Y. Chen, X. Liu, S. Zhang, L. Yang, M. Liu, Y. Zhang and S. Yao, *Electrochim. Acta.*, 231 (2017) 677.
47. M. Zhang, F. Gan and F. Cheng, *Res. Chem. Intermed.*, 42(2) (2016) 813.
48. S.Q. Feng, Y.Y. Zhang and Y.M. Zhong, *J. Electroanal. Chem.*, 733 (2014) 1.
49. F. Hu, S. Chen, C. Wang, R. Yuan, D. Yuan and C. Wang, *Anal. Chim. Acta*, 724 (2012) 40.
50. Y. Umasankar, A.P. Periasamy and S.M. Chen, *Anal. Biochem.*, 411 (2011) 71.

© 2018 The Authors. Published by ESG ([www.electrochemsci.org](http://www.electrochemsci.org)). This article is an open access article distributed under the terms and conditions of the Creative Commons Attribution license (<http://creativecommons.org/licenses/by/4.0/>).